DOI: 10.1002/adma.200701955

Toward the Accurate Read-out of Quantum Dot Barcodes: Design of Deconvolution Algorithms and Assessment of Fluorescence Signals in Buffer**

By *Jeongjin A. Lee*, *Sawitri Mardyani*, *Andy Hung*, *Alex Rhee*, *Jesse Klostranec*, *Ying Mu*, *David Li*, and *Warren C. W. Chan**

Since the introduction of quantum dot (QD) barcoding technology for biological applications in 2001,[1] their development from academic research labs to commercial applications has been slow. Excitement in the concept of QD-barcodes stems from their ability to measure multiple protein and nucleic acid targets simultaneously with high sensitivity.[2–3] Compared to producing barcodes using organic fluorophores, the use of QDs could lead to a greater number of barcodes because of their tuneable emission and narrow spectral linewidth;[4–8] furthermore, QD-barcodes require only a low-power single excitation source due to their large absorption cross-section and continuous absorbance profile, which greatly reduces the complexity and cost of instrumentation. It has been suggested that such a system could rival microarray technologies, which are commonly used for measuring large numbers of biological molecules in a short timeframe.[9–11] Much effort in the last five years has focused on the reproducible synthesis of QD-barcodes.[12–14] The method for reading the QD-barcodes and the impact of environmental conditions on fluorescence stability of the barcodes have been largely ignored. Without considering these two constraints, the accurate identification of the barcodes could be compromised leading to false detection outcomes. The purpose of this manuscript is to explore signal processing methods for deconvolving the fluorescence signals of the QD-barcodes and to use this method to determine a practical number of available barcodes for biological applications. Furthermore, we will describe other chemical constraints that are important in the identification of the QD-barcodes.

Figure 1 shows seven QD-barcodes and their corresponding fluorescence spectra upon a single 488 nm optical excitation. By varying concentrations and emissions of the QDs inside the microbeads, barcodes with unique spectral signatures can be created. The fluorescence spectra of the different emitting QD barcodes are rather close to each other and a method to deconvolve the signal will be required.

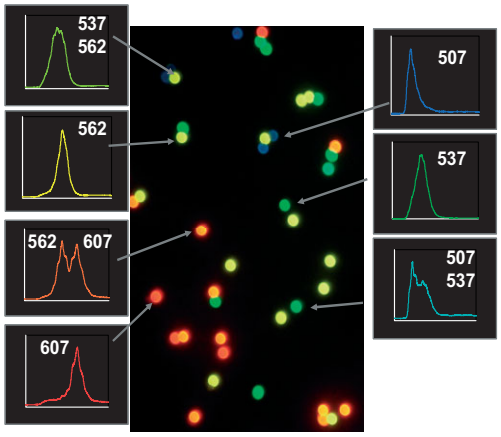

Figure 1. Real-color image of 7 uniquely emitting QD-barcodes and their corresponding spectra. 5 μm QD-barcodes were spread on a glass slide and excited with a Hg lamp (band pass filter of 340 to 360 nm). The fluorescence signal was collected by 40x objective (0.8 N.A.), passed through 430 long pass filter, and imaged using a 35 mm camera. The spectra for the QD-barcodes were acquired in a flowing stream and therefore, the spectra do not appear Gaussian [3]. The spectrum is correlated to the QD-barcode image. The number next to the spectrum indicates the maximum fluorescence emission of the QD-barcodes.

We propose the following strategy to deconvolve the fluorescence spectrum of the barcodes (as described in Fig. 2). This strategy has two steps. Initially (coined as the STEP 1 in Fig. 2), fluorescence emission of single-color QDs used for barcoding is measured by a fluorometer. Gaussian curve modelling of the spectrum data is carried out using the so-called Trust-Region (TR) fitting method.[15–16] The TR-fitting is a non-linear optimization algorithm that minimizes the first two terms of the Taylor approximation to an error function (i.e.,

[*] Prof. W. C. W. Chan, Dr. J. A. Lee, S. Mardyani, A. Hung, A. Rhee, J. M. Klostranec, D. Li
Institute of Biomaterials and Biomedical Engineering
Department of Materials Science and Engineering
The Centre for Cellular and Biomolecular Research
University of Toronto
160 College St., Toronto, ON M5S 3E1 (Canada)
E-mail: warren.chan@utoronto.ca
Prof. Y. Mu
National Laboratory of Industry Control Techniques
Zhejiang University
Hangzhou, Zhejiang 310027 (P.R. China)

[**] This project was funded by Genome Canada through the Ontario Genome Institute. Y.M. acknowledges CSC (22822101) and NSFC (30200050) for visiting fellow support. J.K. and S.M. acknowledge NSERC for student fellowships.

ADVANCED MATERIALS

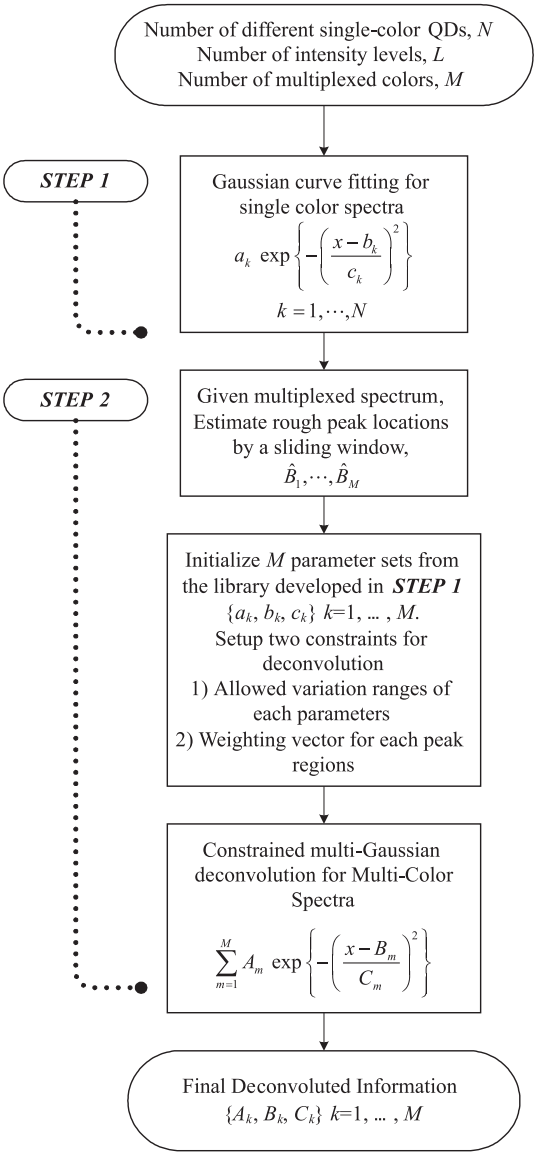

Figure 2. Flow chart describing the deconvolution algorithm for identifying QD-barcodes.

difference between data and objective curve function). Each of the fluorescence spectra is represented by three parametric values called *a*, *b*, and *c* and a library of the Gaussian parameter sets is developed to be used as initial condition in deconvolving barcodes. When barcodes are spectrally read (coined as STEP 2 in Fig. 2), the multiplexed barcode spectra are analyzed in a stepwise-manner by the algorithm. The algorithm is designed so that the read-out of the barcode is rapid without compromising the accuracy. To accomplish this, an initial identification of single-color QD spectra is conducted based on a sliding window method. That is, the number and location of local peaks consisting of the barcode spectrum are first estimated. This is referred to as rough peak locations in Figure 2 as this initial estimation cannot provide exact information of the local peaks in the multiplexed spectrum. Then, two constraints for deconvolution are imposed on the multi-Gaussian TR-fitting for the multiplexed spectrum. These two constraints are; (1) variation ranges of the detected local peak parameter sets {*a*, *b*, *c*} are assigned, and (2) weighing factors for the peak region excluding the background region are given. The constraints play a key role in evaluating accurate local peak information (such as wavelength, emission intensity, width) and they also prevent false identification of barcodes. Optimizing these parameter sets, the spectral signature is deconvolved into a sum of Gaussians, which is translated into a barcode read-out. In other words, this algorithm demixes (or demultiplexes) the spectra into multiple single-color spectra and differentiates the fluorescence spectra of QDs in a mixture or in a barcode.

As an example, in Figure 3, we demonstrate the deconvolution algorithm using QDs of two unique emissions (592 nm and 618 nm) in solution. Initially, the fluorescence spectra of each individual QD is measured and this is depicted in Figure

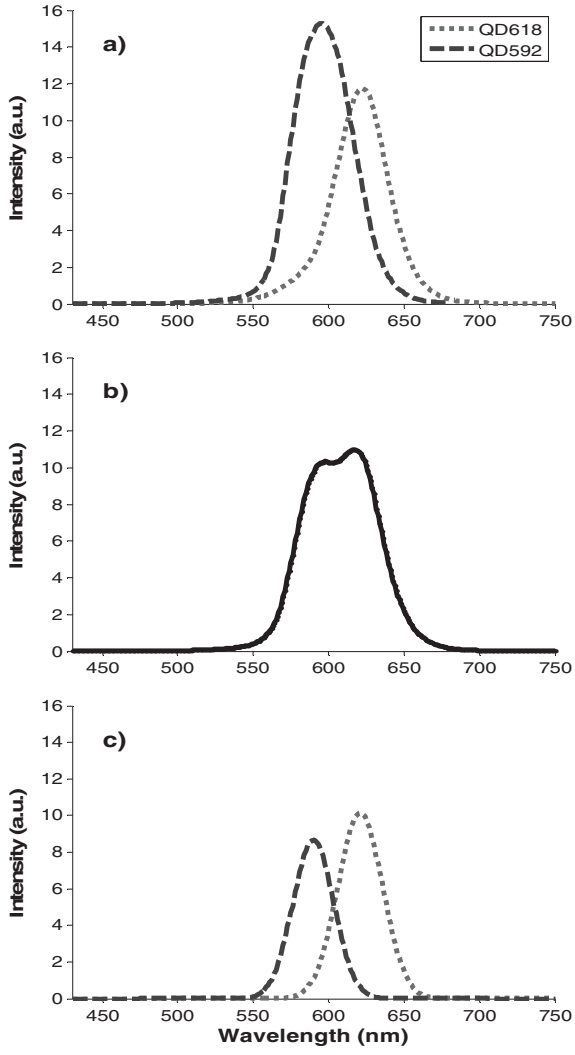

Figure 3. Demixing of QD fluorescence spectra. a) Spectra of two single-color QDs, measured individually. b) Spectrum of two-color QDs in a single solution. c) Deconvolved spectra of the two single-color QDs.

3a. The distance between two peaks is less than 30 nm. When combined in solution, the fluorescence measurement shows a broad fluorescence peak with a range from 550 to 660 nm as shown in Figure 3b. After applying the algorithm, the deconvolved fluorescence peaks (Fig. 3c) have similar appearance to the single QD spectra (Fig. 3a) with similar emission wavelengths but with different intensities. By comparing the peak areas of the deconvolved spectra versus the initial spectra (from Fig. 3), we show that there is only a 0.18% variability after nine iterations. For the other QD-combinations, a variability of less than 0.50% between deconvolved and initial spectra is typically observed. This illustrates the accuracy of the algorithm for deconvolving two fluorescence signals with a large degree of spectral overlap. It is straightforward to generalize this algorithm to the barcodes that have more than two colors. Thus far, we have applied this technique to deconvolve 150 two-color QD combinations in solution spanning 5 intensity levels and using a library of 4 color QDs.

The ability to deconvolve fluorescence spectra addresses an important challenge in QD barcode read-out. The number of discernable QD-barcodes is also dependent upon instrumental measurement error and decoding scheme. We propose two methods of barcode discrimination.

In the first method, the QD barcodes are discriminated based on the intensities of each incorporated QD. We measured the fluorescence of all uniform mixtures of two color QDs in solution, and identified the individual peak intensities by the deconvolution algorithm. At five concentration levels for each of the two-color QD combinations, there could be twenty-five potential barcodes. For example, in Figure 4a, 25 deconvolved intensities of orange-red combination are highlighted in a sequence of O1R1~5, O2R1~5, O3R1~5, O4R1~5, O5R1~5. Orange and red refer to the color of the fluorescence emissions of the QDs and O1R1~5 refers to the mixing of orange-emitting QDs at one defined concentration with five different concentrations of red-emitting QDs to make a set of 5.

We study how the measurement error affects the number of available barcodes by examining the overlapping of fluorescence intensities between the different barcodes of same color combination group. If a barcode is overlapped with any other barcodes, it is screened out due to ambiguity. Using this discrimination method, the final number of unique barcodes for the orange-red combination is 15 out of 25 (with a maximum allowable measurement error of 10%), which are marked with an asterisk in Figure 4a. As a design guideline, the overall usable barcode numbers are plotted against maximum allowable error values in Figure 4b. Clearly, there exists a trade-off between false read-out and the number of usable barcodes. In other words, assays requiring a greater number of barcodes would increase the demand on instrument measurement precision.

The second method that can be used to discriminate QD barcodes is based on the ratio of QD fluorescence intensities. In Figure 5a, we show the use of a ratiometric technique to discriminate between barcodes, again, for the orange-red

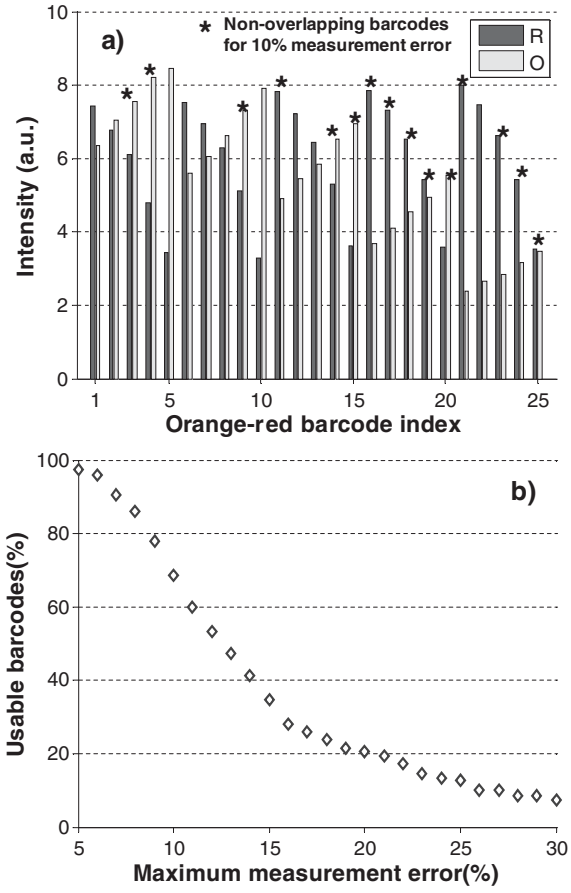

Figure 4. Determining the number of available QD-barcodes using intensity. a) Fluorescence intensities of red-orange QD combinations. b) Using measurement error to dictate the number of usable barcodes for biological assay.

combination. The ratio was obtained by dividing the red peak intensity by the orange peak intensity. Using this technique, the error from measurements becomes negligible if the intensities of each color in a barcode are similarly scaled. Such a situation occurs when bead size and doping yields cannot be precisely controlled. One can set the minimum intensity ratio difference (MIRD) as a criterion to determine the discernability of each barcode from another. For example, if the MIRD is set to be 0.3, only 7 of the 25 barcodes could be used (marked as * in Fig. 5a). Alternatively, if the MIRD reduces to 0.1, the number of available QD-barcodes increases to 14 and conversely a higher MIRD reduces the number of available QD-barcodes. By changing the MIRD criterion, one could alter the reliability of QD-barcode identification. As a design guideline, the overall usable barcode numbers are displayed with different MIRD values in Figure 5b. The ratiometric discrimination scheme demonstrates the possibility of measurement error compensation through the design of read-out algorithm. In general, selecting the appropriate detection scheme to compensate for known sources and patterns of variation in barcode signal can increase read-out reliability.

ADVANCED MATERIALS

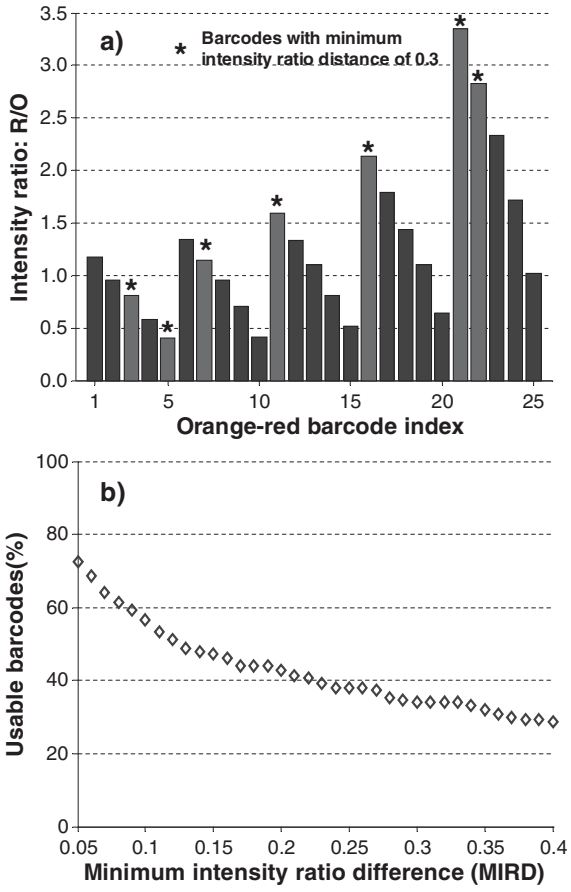

Figure 5. Determining the number of available QD-barcodes by using intensity ratioing. a) Intensity ratio of red-orange QD combinations. b) Using minimum intensity ratio differences to dictate the number of usable barcodes for biological assay.

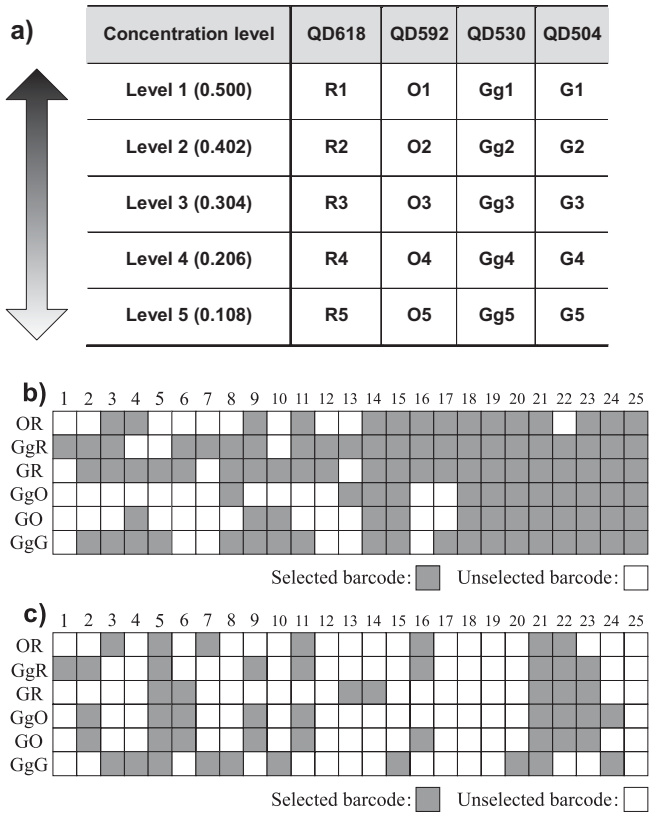

Concentration level	QD618	QD592	QD530	QD504
Level 1 (0.500)	R1	O1	Gg1	G1
Level 2 (0.402)	R2	O2	Gg2	G2
Level 3 (0.304)	R3	O3	Gg3	G3
Level 4 (0.206)	R4	O4	Gg4	G4
Level 5 (0.108)	R5	O5	Gg5	G5

Figure 6. Barcode possibilities of four different emitting QD colors with five intensities. a) Table describing the single-color QD samples. b) Map of the total available barcodes using the intensity value criterion for 10% measurement error. c) Map of the total available barcodes using ratiometric criterion for a minimum intensity ratio difference of 0.3.

By applying the described discrimination methods to the 150 possible two-color barcodes produced from 20 QD samples in Figure 6a, we determine a practical number of available barcodes for use in high-throughput multiplex detection applications. Using the absolute intensity criterion and assuming a measurement error of 10%, 69% (103 out of 150) of the entire barcode set can be used (Fig. 6b). Using the ratiometric method and a MIRD value of 0.3, 34% (51 out of 150) of the entire barcode set can be used (Fig. 6c). This analysis can be easily generalized to a greater number of barcodes built from more extensive libraries and determine the maximum number of practical QD-barcodes available for use in assays.

In addition to overall detection algorithm, environmental factors may also impact the accuracy of QD-barcode identification. QD-barcodes were prepared by diffusing hydrophobic QDs into the microbeads. The QDs are maintained inside the microbeads by hydrophobic-hydrophobic interactions. For these studies, they were not chemically sealed with silane chemistry, as described by Han and co-workers.[1] We found that the sealant could add a variable to these studies since the thickness of the sealant is difficult to properly control. In Figure 7, we show the effect of buffer type and pH on the fluorescence of QDs inside microbeads. We discovered that the buffer used for storage and for conducting assays could influence the optical signals of QD-barcodes. Three different colors of QDs were shown to change fluorescence intensity in the four different buffers. The intensity is the lowest in PBS, followed by carbonate, tris, and HEPES buffer. There is a large difference, however, in the magnitude of variation. Fluorescence varies 122.0 ± 32.2 %, 91.0 ± 43.1 % and 691.0 ± 47.5 % in QD528, QD565 and QD585, respectively. Figure 7b shows QD585 has much larger variation range compared to QD528 and QD565. This has also been observed by Boldt et al.,[17] who found that larger quantum dots are less stable towards their chemical environment than smaller ones. Although the difference between our study and Boldt et al.'s study is the QDs used in our experiments are capped with a ZnS-layer while Boldt et al. used uncapped CdSe QDs. Despite the initial belief that the ZnS-layer protected the CdSe QDs from environmental effects,[18] it has been shown recently that the ZnS-capping does not prevent the fluctuations in the fluorescence of the CdSe qdots in aqueous buffer.[19] The surface area of the CdSe core of QD585 is 141% greater than QD528 and 55% greater than QD565. This greater surface area allows for more interaction between the QD and the

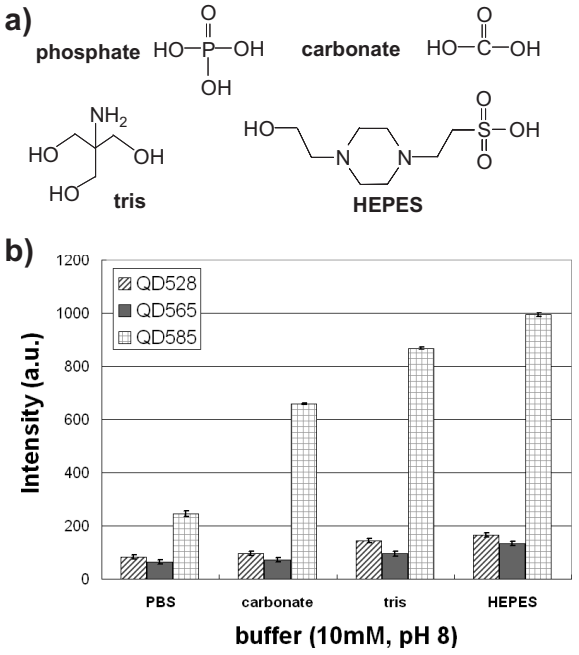

Figure 7. Effect of buffer molecules on the fluorescence of QD-barcodes. a) Chemical structures of the main molecules in the buffers used in this study. b) Variation in fluorescence intensity of different colored (green(QD528), yellow(QD565) and orange (QD585)) QDs in four commonly used biological buffers, at the same concentration (10 mM) and pH 8. In all these QDs, the fluorescence in PBS < carbonate < tris < HEPES. QD585 shows the greatest degree of variation in fluorescence among the four buffers. Error bars indicate the 95% confidence interval on the mean normalized fluorescence.

environment, thereby increasing the effect of the QD's chemical environment on the intensity of its fluorescence.

Figure 8 shows the fluorescence intensities of green-emitting QD528 with different amounts of ZnS capping (QD528a < QD528b < QD528c) in citrate buffer of pH 5 – pH 7. This range is significant because it's used in many biological assays.

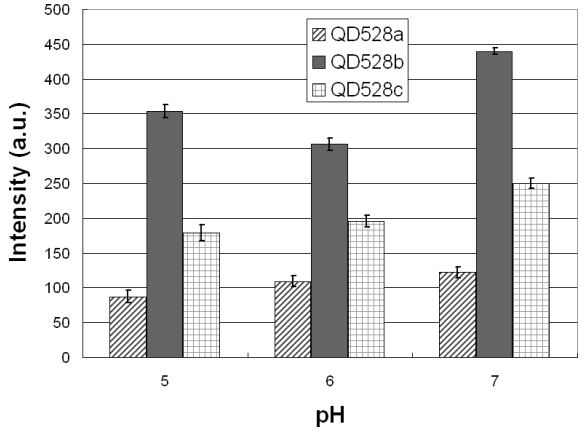

Figure 8. Variation in fluorescence intensity of green QD528 with different amounts of ZnS capping in citric acid buffer, pH 5–7. Generally, QDs showed higher fluorescence in higher pH buffers.

The fluorescence of the QDs was found to increase with increasing pH. This trend of increasing fluorescence of QDs with increasing pH is also seen with other buffers including tris, HEPES, PBS and borate. In 10mM citric acid, these green QDs showed between 40–43% change in fluorescence between pH 5~7. Yellow and orange-emitting QDs with different amount of ZnS capping varied in fluorescence between 22% – 345% in citrate buffer with a pH of 5~7. This large variation only underlines the necessity to study these variations before QDs are used in quantitative applications, as what is seen in one sample of QDs may not necessarily be repeated in another sample. In all the studies described above, UV-vis spectroscopy did not show any QDs in the supernatant, indicating that the variation in fluorescence intensity was not due to leakage of QDs from the microbeads. Typically, the QDs do not significantly leak out of the microbeads after 1 to 2 days of preparing the QD-barcodes.

However, for the Qd-barcode shelf-life, several factors affect their fluorescence signals: (1) the QDs could leak out of the microbeads when they are stored in solution for long-term (> 2 days) and are not properly sealed and (2) the QDs could photobrightening due to photo-oxidation or capping-ligand interactions.

Because of these fluctuations in QD signals inside microbeads, the use of absolute intensity as a barcode discrimination method could lead to mis-identification of the QD-barcodes. Even though the ratiometric method leads to a decreased availability of barcodes compared to the absolute intensity method, it may lead to more accuracy with less false identifications. The ratiometric intensity is a more robust criterion because it takes into account of factors that cause variation. For example, in Figure 7b, the absolute intensities of green-(QD528), yellow-(QD565), orange-(QD585) emitting QDs show substantial variations: 32.2 %, 43.1 %, and 47.5 %, respectively, in different buffers. Using a ratiometric intensity of yellow/green-emission, however, we can reduce the variation as low as 8.5 %, which means that the ratiometric method could be more reliable than the absolute intensity method.

We conclude that read-out algorithms and environmental factors determine the number of available QD-barcodes for use in biological assays. Despite the proposed feasibility to synthesize > 1 million barcodes from a library of 6 colors and 10 intensity levels, we have shown practical limitations from the read-out algorithm point of view. Based on the method of discrimination, the practically discernable number of barcodes is determined. We provided a design of an algorithm to deconvolve the fluorescence spectra of multiple QDs and developed two strategies to differentiate the QD signals when multiple-emitting QDs are mixed in solution. These parameters imposed by the decoding system could be used to direct the design of QD-barcodes for high accuracy read-out. In the future, more complex algorithms will be required to take into account the variability in fluorescence emission of QDs in biological environment, which could further limit the number of available barcodes. Despite the challenges, this technology is still early in its development and solving these problems could

ADVANCED MATERIALS

extend this technology toward many biological and medical applications that cannot be achieved using current state-of-the-art detection systems.

Experimental

Synthesis of ZnS-capped CdSe Nanocrystals. ZnS-capped, CdSe QDs were synthesized using a previously described organometallic procedure.[18,20,21] The green (504, 528, 530 nm emissions), yellow (565 nm emission), orange (585, 592 nm emissions) and red (618 nm emission) CdSe QD cores were made in three separate reactions. The green, yellow, orange, and red description refers to the fluorescence color emission of the QDs. In each reaction, once the core was made, the vessel was cooled to 270 °C and the capping solution (consisting of diethylzinc and hexamethyldisilathiane in tri-n-octylphosphine) was added to produce the ZnS capping layer on the CdSe core. To make QDs with the same core but different capping thickness, aliquots were taken after the addition of 1.0 ml, 2.0 ml, 3.0 ml of capping solution (0.232 M diethyl zinc, and 0.162 M hexamethyl disilathiane), corresponding to QD528a, QD528b, QD528c, respectively in Figure 8. ICP-AES was used for analysis of QD composition.

Preparation of QD-barcodes. QD-barcodes are prepared by using a two-step method: (1) polystyrene microbeads are either synthesized in-house or purchased and (2) tri-n-ocytlphosphine oxide coated ZnS-capped CdSe QDs is mixed with polystyrene microbeads.[1] We recognize that there are many methods to prepare QD-barcodes; however, the Nie method was used because it is the simplest way to prepare the barcodes and it provides barcodes with the highest microbead size uniformity. Spectra were taken of microbeads flowing in a polydimethylsiloxane (PDMS) microfluidic channel (100 μm wide by 15 μm high) using electrokinetics. QDs in the beads were excited using a 488 nm Ar laser line at 25 mW, focused to an 8 μm spot size using a 60X oil immersion objective (1.35 NA). Fluorescence was collected using the same objective, dispersed using a grating and the spectrum measured using a thermo-electrically cooled CCD array camera [3]. Integration time of the camera was set to 50 msec. Background signals were subtracted.

Preparing QDs for Demixing Experiment. Concentrations of the constituents of four color groups were controlled based on the absorbance value at the quantum-confinement peak wavelength[22]. The highest single-color QD solution samples (named R1, Y1, Gg1, and G1 in the 'Level 1' row) had an equal absorbance value of 0.50. Serial dilution using chloroform was conducted to obtain other concentrations. The two color multiplexing out of the four colors (corresponding to $N = 4$, $L = 5$, $M = 2$ in Figure 2) yields 6 different two-color combinations, i.e., RY, RGg, RG, YGg, YG, GgG, and each of 25 combinations producing distinct QD barcodes were prepared by mixing them together at a 1:1 ratio. All spectra were measured by Fluoromax-3.

Environmental Effects on QD-barcode Fluorescence. The QD-barcodes were washed three times in propanol, dried and re-suspended in aqueous buffers of various concentrations and pH. They were incubated overnight at room temperature and then the fluorescence intensity was measured through flow cytometry. A Coulter Epics XL flow cytometer was used to measure the fluorescence of the QD-barcodes in various buffers. The flow cytometer measured the fluorescence emission, side scatter and forward scatter of 10000 particles in each sample. As some of these particles may be aggregates of microbeads, broken microbeads, or aggregates of quantum dots, forward scatter and side scatter, which can be correlated to the size and granularity of particles were used to single out the population of monodisperse microbeads from larger aggregates and smaller particles. Only the fluorescence of single QD-barcodes was used in further analysis to calculate the mean and confidence interval for the fluorescence of each type of QD in the different buffers.

Received: August 3, 2007

[1] M. Han, X. Gao, J. Z. Su, S. Nie, *Nat. Biotech.* **2001**, *19*, 631.
[2] H. Xu, M. Sha, E. Y. Wong, J. Uphoff, Y. Xu, J. A. Treadway, A. Truong, E. O'Brien, S. Asquith, M. Stubbins, N. K. Spurr, E. H. Lai, W. Mahoney, *Nucleic Acids Res.* **2003**, *31*, e43.
[3] J. M. Klostranec, Q. Xiang, G. A. Farcas, J. A. Lee, A. Rhee, E. I. Lafferty, S. D. Perrault, K. C. Kain, W. C. W. Chan, *Nano Lett.* **2007**, *7*, 2812.
[4] M. Bruchez, M. Moronne, P. Gin, S. Weiss, A. P. Alivisatos, *Science* **1998**, *281*, 2013.
[5] W. C. W. Chan, S. Nie, *Science* **1998**, *281*, 2016.
[6] A. P. Alivisatos, *J. Phys. Chem.* **1996**, *100*, 13226.
[7] I. L. Medintz, H. T. Uyeda, E. R. Goldman, H. Mattoussi, *Nat. Mater.* **2005**, *4*, 435.
[8] J. M. Klostranec, W. C. W. Chan, *Adv. Mater.* **2006**, *18*, 1953.
[9] R. F. Service, *Science* **1998**, *282*, 396.
[10] D. Gershon, *Nature* **2005**, *437*, 1195.
[11] M. Eisenstein, *Nature* **2006**, *444*, 959.
[12] X. Gao, S. Nie, *Anal. Chem.* **2004**, *76*, 2406.
[13] T. R. Sathe, A. Agrawal, S. Nie, *Anal. Chem.* **2006**, *78*, 5627.
[14] N. Gaponik, I. L. Radtchenko, G. B. Sukhorukov, H. Weller, A. L. Rogach, *Adv. Mater.* **2002**, *14*, 879.
[15] J. J. More, D. C. Sorensen, *SIAM J. Sci. Stat. Comp.* **1983**, *4*, 553.
[16] M. A. Branch, T. F. Coleman, Y. Li, *SIAM J. Sci. Comp.* **1999**, *21*, 1.
[17] K. Boldt, O. T. Bruns, N. Gaponik, A. Eychmuller, *J. Phys. Chem. B* **2006**, *110*, 1959.
[18] M. A. Hines, P. Guyot-Sionnest, *J. Phys. Chem.* **1996**, *100*, 468.
[19] J. A. Kloepfer, S. E. Bradford, J. L. Nadeau, *J. Phys. Chem. B.* **2005**, *109*, 9996.
[20] B. O. Dabbousi, J. Rodriguez-Viejo, F. V. Mikulec, J. R. Heine, H. Mattoussi, R. Ober, K. F. Jensen, M. G. Bawendi, *J. Phys. Chem. B* **1997**, *101*, 9463.
[21] X. Peng, M. C. Schlamp, A. V. Kadavanich, A. P. Alivisatos, *J. Am. Chem. Soc.* **1997**, *119*, 7019.
[22] W. C. W. Chan, D. J. Maxwell, X. Gao, R. E. Bailey, M. Han, S. Nie, *Curr. Opin. Biotech.* **2002**, *13*, 40.